Reconstruction Of A Compactly Supported Function From The Discrete Sampling Of Its Fourier Transform*

Jiahong Yin, Alvaro R. De Pierro
Dept. Applied Math., State University of Campinas, 13083-970 SP, Brazil
Tel: 55-19-788-7915, FAX: 55-19-239-7915
e-mail: alvaro@ime.unicamp.br
Musheng Wei
Dept. Math., East China Normal University, Shanghai 200062, China
Tel: 86-21-6245-7495
e-mail: mwei@math.ecnu.edu.cn

March 8, 2001

Abstract. We derive a new relation between the Discrete Fourier Transform of a discrete sampling set of a compactly supported function and its Fourier transform. From this relation we obtain a new window function. We then propose a new efficient algorithm to reconstruct the original function from the discrete sampling of its Fourier transform, which can adopt the fast Fourier transform and has much better accuracy than those in the literature. Several numerical experiments are also provided to demonstrate the results.

EDICS numbers: SP 2.1, SP 2.5.3

*The first author was supported by FAPESP grant No. 96/000837-0 , Brazil, the second by FAPESP grant No. 1996/2758-0, and CNPq grant No. 301699-81, Brazil, and the third author by the National Natural Science Foundation, P. R. China and FAPESP grant No. 1996/2758-0, Brazil.

1. Introduction

The Fourier Transform (FT) is a powerful tool for scientific computation which is found in numerous applied areas [3],[11]. For example, in image reconstruction, from a set of line integrals of the density of an object we get a discrete sampling of the Fourier transform of the density by applying the Fourier slice theorem [9]. So we need to reconstruct the values of the density at some discrete set of points in the object. The Fourier method is one of the tools to achieve this aim. It is clear that we can exactly reconstruct a compactly supported function from all the values of its Fourier transform. However, when we only know a discrete set of values, how can we recover some discrete values of the original function? For simplicity, in this paper we only discuss the case that the density $f(\cdot)$ is a function of one variable $x \in R = (-\infty, +\infty)$, but the results can be easily extended to the multi-dimensional case.

From a mathematical point of view, this problem can be described as follows. We first make the following assumptions.

Assumptions. The function $f(x)$ satisfies

1. $f(\cdot)$ is defined for every $x \in R$, $\in L^2(R)$; $f(x) = 0$ for $x \notin [0,1]$ and $\sup_{x\in[0,1]}|f(x)| \leq C$, where $C > 0$ is a constant.

2. $f(x)$ has at most a finite number of points of discontinuity $z_1, \cdots, z_l$ and they are given.

3. For $x \notin Z = \{z_1, \cdots, z_l\}$, $f'(x)$ exists and $\sup_{x\notin Z}|f'(x)| \leq C$.

Assumptions 1-3 are realistic in practical problems. In another paper, we discuss the case with unknown points of discontinuity. If the support of $f(x)$ is in the interval $[a,b] \neq [0,1]$, then we can use a linear transformation $\xi = \frac{x-a}{b-a}$ to change the support to $[0,1]$.

The Fourier transform and inverse Fourier transform of $f(x)$ are respectively defined as

$$\hat{f}(\omega) = \int_{-\infty}^{+\infty} f(x)e^{-i2\pi x\omega}dx = \int_{0}^{1} f(x)e^{-i2\pi x\omega}dx \tag{1}$$

and

$$f(x) = \int_{-\infty}^{+\infty} \hat{f}(\omega)e^{i2\pi x\omega}d\omega, \ a.e. \tag{2}$$

Because $f(x)$ is compactly supported in $[0,1]$, $\hat{f}(\omega)$ is sufficiently smooth (Paley-Wiener's Theorem, [2]). Notice that in this case, the support of $\hat{f}(\omega)$ is R.

Let

$$0 = x_0 < x_1 < \cdots < x_{N-1} < x_N = 1, \quad \Delta x_j = x_{j+1} - x_j = \Delta x = \frac{1}{N} \tag{3}$$

and

$$f_j = f(\eta_j),\ j = 0, \ldots, N-1 \text{ with } \eta_j = x_j + \delta, \tag{4}$$

where $0 \leq \delta \leq \Delta x$ is a constant.

One approach to obtain approximate values of $\{f_j,\ j = 0, \ldots, N-1\}$ is as follows. Suppose that when $|\omega|$ is sufficiently large, there exists a positive constant W such that when $|\omega| \geq W$, the corresponding interval in the integral (2) can be ignored. Then one has that

$$f(x) \approx \int_{-W}^{W} \hat{f}(\omega) e^{i2\pi x\omega} d\omega, 0 \leq x \leq 1. \tag{5}$$

Approximating the integral (5) by a Riemann sum, one has [4]

$$f_j \approx \sum_{k=0}^{M-1} \hat{f}(\omega_k) e^{-i2\pi\eta_j\omega_k} \Delta\omega_k, j = 0, \ldots, N-1, \tag{6}$$

where

$$-W = \omega_0 < \omega_1 < \cdots < \omega_{M-1} < \omega_M = W, \ and \ \ \Delta\omega_k = \omega_{k+1} - \omega_k = \Delta\omega = \frac{2W}{M}.$$

Because of the fact that the integral (5) is approximated by the Riemann sum (6), one can get a good approximation only for small $\Delta\omega$ and so M must be large for a fixed W, and one needs a large number of sampling values of $\hat{f}(\omega_k)$. On the other hand, one wants to apply the fast Fourier transform (FFT) to reduce the amount of computations, and this implies taking the maximal frequency $W = \frac{1}{2\Delta x}$ and choosing $M = N$. In the case that the support of $f(x)$ is $[0,1]$, $\Delta\omega = \frac{2W}{M} = 1$, so using the Riemann sum (6) will result in large error. If one takes $\Delta\omega = O(\Delta x) = O(\frac{1}{N})$ and $W = \frac{1}{2\Delta x}$, then the amount of computations would be $O(N^3)$, it would be prohibitively large for large N.

Another approach to obtain approximate values of $\{f_j,\ j = 0, \ldots, N-1\}$ is for the case that the support of $f(x)$ is $[a, b]$, with $A = b - a > 1$, see, e.g, [11]. In this case, (2) is replaced by

$$\hat{f}(\omega) = \int_{-\infty}^{+\infty} f(x) e^{-i2\pi x\omega} dx = \int_{a}^{b} f(x) e^{-i2\pi x\omega} dx \tag{7}$$

and the nodes $\{x_k\}$ are defined as

$$a = x_0 < x_1 < \cdots < x_{N-1} < x_N = b, \quad \Delta x_j = x_{j+1} - x_j = \Delta x = \frac{A}{N}.$$

Then in the Riemann sum (6) one chooses $W = \frac{1}{2\Delta x}$ and $M = N$ allowing the application of the FFT. In this case, $\Delta\omega = \frac{1}{A}$ and $\Delta x = \frac{A}{N}$ so the sampling interval $\Delta\omega$ depends on the support of $f(x)$ and using the Riemann sum (6) will also result in large error. To get a good approximation of the problem, several types of window functions are used to reduce the error [8], [3]. In §3 we list some widely used window functions.

In this paper we derive a new relation between the discrete Fourier transform of a discrete sampling set of $f(x)$ and its Fourier transform. From this relation we obtain a new window function that gives rise to a new efficient algorithm to reconstruct the original function from the discrete samplings of its Fourier transform. With this new approach the FFT can be used and much better accuracy than that previously obtained in the literature is achieved.

The paper is organized as follows. Section 2 lists some formulae of the discrete Fourier transform of a discrete sampling values $\{f_j,\ j = 0, 1, \cdots, N-1\}$ of the function $f(x)$, the Fourier transform of $f(x)$ with the frequency k, and the Fourier expansion of $f(x)$ if we just consider that $f(\cdot)$ is defined over its support $[0, 1]$; Section 3 derives a new approximate relation between the Fourier transform with frequency k and the discrete Fourier transform; from this relation the new window function σ_k is deduced; Section 4 presents our algorithms for the reconstruction of $\{f_j, j = 0, 1, \cdots, N-1\}$ from a discrete sampling of its Fourier transform $\{\hat{f}_k,\ k = -N/2, , \cdots, N/2 - 1\}$; Section 5 shows several numerical experiments that illustrate the advantages of the new approach; Section 6 concludes the paper with some remarks.

2. The Discrete Fourier Transform, the Fourier Transform and the Fourier Expansion

The goal of this paper is to derive an approximate relation between the discrete Fourier transform and Fourier transform with frequency k of the function $f(x)$, so that we can use the FFT to evaluate $\{f_j, j = 0, \cdots, N-1\}$ efficiently and accurately. In this section we highlight some results and motivation for the discrete Fourier transform, the Fourier transform and the Fourier expansion.

1. The discrete Fourier transform:

For a given function $f(x) \in L^2(R)$ with support in $[0,1]$ and an even integer $N > 0$, let $\{x_j,\ j = 0, \cdots, N-1\}$ and $\{f_j,\ j = 0, \cdots, N-1\}$ be defined as in (3) and (4), respectively. Then the discrete Fourier transform of $\{f_j,\ j = 0, \cdots, N-1\}$ is

$$\tilde{f}_k = \frac{1}{N} \sum_{j=0}^{N-1} f_j e^{-i2k\pi \frac{j}{N}}, -N/2 \leq k \leq N/2 - 1 \tag{8}$$

and the inverse formula is:

$$f_j = \sum_{k=-N/2}^{N/2-1} \tilde{f}_k e^{i2k\pi \frac{j}{N}}, j = 0, \ldots, N-1. \tag{9}$$

The discrete Fourier transform is the mapping between the N complex numbers $\{f_j, j = 0, \ldots, N-1\}$ and the N complex numbers $\{\tilde{f}_k, k = -N/2, \ldots, N/2-1\}$. We can use the fast Fourier transform (FFT) to compute them.

2. The Fourier transform with frequency k:

For a given function $f(x) \in L^2(R)$ with support in $[0,1]$, its Fourier transform is given in (1). From (8) and (9), in order to establish the relation between the discrete Fourier transform and the Fourier transform of $f(x)$, we just need to establish the relation between the discrete Fourier transform and the Fourier transform with frequency k. From (1) we obtain

$$\hat{f}_k \equiv \hat{f}(k) = \int_0^1 f(x) e^{-i2k\pi x} dx,\ k = 0, \pm 1, \pm 2, \ldots. \tag{10}$$

If f is a real valued function, $\hat{f}_{-k} = \overline{\hat{f}_k}$.

3. The Fourier expansion:

The set of functions $\{e^{i2k\pi x}, k = 0, \pm 1, \pm 2, \ldots\}$ is an orthogonal system over the interval [0,1]. Because the support of $f(x)$ is in the interval $[0, 1]$, we can also consider $f(x)$ as defined on [0,1], and we can obtain the Fourier expansion of $f(x)$:

$$Sf(x) = \sum_{k=-\infty}^{+\infty} c_k e^{i2k\pi x} \tag{11}$$

with the Fourier coefficients

$$c_k = \int_0^1 f(x) e^{-i2k\pi x} dx, \ \ k = 0, \pm 1, \pm 2, \ldots . \tag{12}$$

$Sf(x)$ represents the formal expansion of f in terms of the Fourier orthogonal system $\{e^{i2k\pi x}, k = 0, \pm 1, \pm 2, \ldots\}$. If f is a real valued function, $c_{-k} = \overline{c_k}$.

Notice that the Fourier coefficient c_k in (12) is exactly the same as $\hat{f}_k$, the Fourier transform of $f(x)$ with frequency k in (10).

The truncated Fourier expansion of $f(x)$ is

$$P_N f(x) = \sum_{k=-N/2}^{N/2-1} c_k e^{i2k\pi x} \tag{13}$$

Equation (13) is different from the theoretical discussion of truncated Fourier transform, but it corresponds directly to the way in practical computation is actually programmed.

In order to make this expansion rigorous, one has to cope with some problems: when and in what sense is the transform convergent, what is the relation between the transform and the function $f(x)$, and how rapidly does the series converge. It is well known that if $f(x) \in C^\infty(0, 1)$ and $f^{(p)}(0) = f^{(p)}(1)$ for all $p = 0, 1 \cdots$, then

$$P_N f(x) \to f(x) \text{ exponentially for } N \to \infty, \ \forall x \in [0, 1].$$

But when $f(x)$ has points of discontinuity, or even when $f(x) \in C^\infty(0, 1)$ but is not periodic, then the convergence is poor and the Gibbs phenomenon occurs. In this case, one needs to

use window functions (also called smoothing functions) to reduce oscillations nearby points of discontinuity [8], [5], [3]. [6] proposes another approach to this problem.

3. A New Relation Between $\hat{f}_k$ And $\tilde{f}_k$. A New Window Function

In this section we will derive a new approximate relation between $\hat{f}_k$ and $\tilde{f}_k$ from which we will be able to provide a new window function to reduce the error when performing the FFT to evaluate $\{f_j,\ j = 0, \cdots, N-1\}$. We first present the main theoretical results of this section.

Theorem 1. Suppose that the function $f(x)$ satisfies Assumptions 1-3, $\{x_j\}_0^N$ and $\{f_j\}_0^{N-1}$ are defined as in (3) and (4) respectively, and $z_k \in \{x_j\}_1^{N-1}, k = 1, \ldots, l$. Then

$$|\hat{f}_k - a_k \tilde{f}_k| \leq C(f)\Delta x \tag{14}$$

where

$$a_k = \begin{cases} 1, & k = 0, \\ \frac{N(e^{-i2k\pi/N}-1)}{-i2k\pi} = \frac{\sin(k\pi/N)}{k\pi/N} e^{-ik\pi/N}, & k \neq 0, \end{cases} \tag{15}$$

and $C(f)$ is a nonnegative constant depending upon f.

Proof: We first prove the case that $k \neq 0$. For the partitions of the nodes $\{x_j,\ j = 0, 1, \cdots, N-1\}$ defined in (3) and the discrete values $\{f_j,\ j = 0, 1, \cdots, N-1\}$ defined in (4) we have (notice that $x_j = \frac{j}{N}$)

$$\int_{x_j}^{x_{j+1}} e^{-i2k\pi x} dx = \frac{e^{-i2k\pi x}}{-i2k\pi}|_{x_j}^{x_{j+1}} = e^{-i2k\pi\frac{j}{N}} \frac{e^{-i2k\pi/N} - 1}{-i2k\pi},$$

from which we obtain

$$\int_{x_j}^{x_{j+1}} e^{-i2k\pi x} dx = \frac{a_k}{N} e^{\frac{-i2k\pi j}{N}}. \tag{16}$$

Notice that the above equality also holds when $k = 0$. We then use the rectangular rule for the approximation of integral to obtain

$$\hat{f}_k = \sum_{j=0}^{N-1} \int_{x_j}^{x_{j+1}} f(x) e^{-i2k\pi x} dx = \sum_{j=0}^{N-1} f_j \int_{x_j}^{x_{j+1}} e^{-i2k\pi x} dx + r_k(\Delta x),$$

where $r_k(\Delta x)$ is the error term to be specified later. So

$$\hat{f}_k = \sum_{j=0}^{N-1} f_j e^{-i2k\pi \frac{j}{N}} \frac{e^{-i2k\pi/N} - 1}{-i2k\pi} + r_k(\Delta x).$$

Since

$$\tilde{f}_k = \frac{1}{N} \sum_{j=0}^{N-1} f_j e^{-i2k\pi \frac{j}{N}}, -N/2 \le k \le N/2 - 1,$$

we have

$$\hat{f}_k = \tilde{f}_k \frac{N(e^{-i2k\pi/N} - 1)}{-i2k\pi} + r_k(\Delta x) = a_k \tilde{f}_k + r_k(\Delta x). \tag{17}$$

Now we turn to estimate the term $r_k(\Delta x)$. Suppose that the derivative of $f(x)$ exists in the subinterval (x_j, x_{j+1}), then for any $x \in (x_j, x_{j+1})$ we have that

$$f(x) = f_j + f^{'}(\xi)(x - \eta_j), \text{ for some } \xi \in (x_j, x_{j+1})$$

and using (15), (16) and Assumption 3 we get

$$|\int_{x_j}^{x_{j+1}} (f(x) - f_j) e^{-i2k\pi x} dx| \le \int_{x_j}^{x_{j+1}} \sup_{\xi} |f^{'}(\xi)| |(x - \eta_j)| dx \le \frac{1}{2} C(\Delta x)^2,$$

where C is defined in Assumption 1. If we choose η_j as $x_j + \Delta x/2$, the bound above will be $\frac{1}{4} C(\Delta x)^2$.From the above inequality and from (8), (10), (15), (16) and (17), we obtain

$$\begin{aligned} |r_k(\Delta x)| = |\hat{f}_k - a_k \tilde{f}_k| &\le \sum_{j=0}^{N-1} \int_{x_j}^{x_{j+1}} |f(x) - f_j| dx \\ &\le N \tfrac{1}{2} C(\Delta x)^2 \equiv C(f) \Delta x, \end{aligned} \tag{18}$$

In the case that $k = 0$, then the value of integral (16) is $1/N$. Following the proof for the case $k \neq 0$, we can easily obtain the same estimate (14) with $a_0 = 1$. Thus we complete the proof of the theorem.

The following remarks are in order.

1. Let $\sigma_k = \frac{1}{a_k}$. Then we have from (15)

$$\sigma_k = \begin{cases} 1, & k = 0, \\ \frac{k\pi/N}{\sin(k\pi/N)} e^{ik\pi/N}, & k \neq 0, \end{cases} \tag{19}$$

and it can be verified that

$$1 \leq |\sigma_k| \leq \frac{\pi}{2}$$

from the well known inequality

$$\frac{2}{\pi} \leq \frac{\sin\theta}{\theta} \leq 1 \quad \text{for} \quad 0 < \theta \leq \frac{\pi}{2}.$$

2. When computing the approximate values $\{f_j,\ j = 0, 1, \cdots, N-1\}$ using the FFT, we use the approximate values for $\tilde{f}_k$:

$$\tilde{f}_k \approx \sigma_k \hat{f}_k \quad k = -N/2, \cdots, N/2 - 1. \tag{20}$$

Notice that σ_k is a window function. There are other well known window functions (see, e.g, [8], pp. 532-538, [3], pp. 45-53[1]):

(a). The Lanczos' window function $\sigma_k^{(1)} = \begin{cases} 1, & k = 0, \\ \frac{\sin(k\pi/N)}{k\pi/N}, & k \neq 0, \end{cases}$.

(b). The Raised Cosine window function $\sigma_k^{(2)} = \frac{1+\cos(k\pi/N)}{2}$.

(c). The Cesáro's window function $\sigma_k^{(3)} = 1 - |k|/(N/2+1)$.

All these three window functions are real. The main reason to introduce these window functions is to reduce oscillations nearby the points of discontinuity, and the accuracy is a secondary consideration.

The magnitude of the window function σ_k is the inverse of the Lanczos' window function, and σ_k also has a phase change $e^{ik\pi/N}$. We claim that our window function is the best one, in the sense that with this window function we establish an accurate relation between $\tilde{f}_k$ and

[1] In the formulae of [3], $\sigma_k^{(1)} = \frac{\sin(2k\pi/N)}{2k\pi/N}$ and $\sigma_k^{(2)} = \frac{1+\cos(2k\pi/N)}{2}$. We find in our computations that the window functions $\sigma_k^{(1)}$ and $\sigma_k^{(2)}$ without the factor two are better.

$\hat{f}_k$ via formula (14). Furthermore, we can obtain a very good approximation for functions $f(x)$ containing points of discontinuity and/or $f(1) \neq f(0)$.

3. In two special cases, we even obtain astonishing results (exact recovery of $\{f(\eta_j) = f_j\}_0^{N-1}$), as shown by the following corollaries.

Corollary 1. Suppose that $f(x)$ is a step function supported in $[0,1]$. Let $\{x_j\}_0^N$ and $\{f_j\}_0^{N-1}$ be defined by (3) and (4) respectively, such that all interior points of subinterval (x_j, x_{j+1}) are not points of discontinuity for $j = 0, 1, \cdots, N-1$. If $f_j = f(\eta_j) = f(x_j + \delta)$ with $0 < \delta < \Delta x$, then

$$a_k \tilde{f}_k = \hat{f}_k \quad k = -N/2, \cdots, N/2 - 1, \tag{21}$$

and so by using the inverse FFT from $\{\sigma_k \hat{f}_k\}_{-N/2}^{N/2-1}$ we recover the values f_j exactly.

Proof. In the estimation of $r_k(\Delta x)$ in formula (18) of Theorem 1, we have $C = 0$ under the condition of the corollary. So $r_k(\Delta x) = 0$ therefore

$$\tilde{f}_k = \sigma_k \hat{f}_k \quad k = -N/2, \cdots, N/2 - 1,$$

completing the proof of the corollary.

Corollary 2. Suppose that $f(x)$ is a function with support in $[0,1]$, such that $f(x) = \alpha x + \beta$ for $x \in [0,1]$. Let $\{x_j\}_0^N$ and $\{f_j\}_0^{N-1}$ be defined in (3) and (4) respectively. If $f_j = f(\eta_j) = f(x_j + \Delta x/2)$, then

$$\hat{f}_k = a_k \tilde{f}_k \quad k = -N/2, \cdots, N/2 - 1, \tag{22}$$

and so by using the inverse FFT from $\{\sigma_k \hat{f}_k\}_{-N/2}^{N/2-1}$ we recover the values f_j exactly.

Proof. Under the conditions of the corollary, for $k = -N/2, \cdots, N/2 - 1$, we have by integrating by parts

$$\int_{x_j}^{x_{j+1}} (f(x) - f_j) e^{-i2k\pi x} dx = B_k \alpha e^{-i2k\pi j/N}, \quad B_k = \begin{cases} 0, & k = 0, \\ i(\frac{\cos(k\pi/N)}{2kN\pi} - \frac{\sin(k\pi/N)}{4k^2N\pi^2}), & k \neq 0. \end{cases}$$

Notice that B_k is independent of j. So substituting the above identity into the formula for

$r_k(\Delta x)$ in the proof of Theorem 1, we obtain for $k = -N/2, \cdots, N/2 - 1$,

$$r_k(\Delta x) = \hat{f}_k - a_k \tilde{f}_k = \sum_{j=0}^{N-1} \int_{x_j}^{x_{j+1}} (f(x) - f_j) e^{-i2k\pi x} dx$$
$$= B_k \alpha \sum_{j=0}^{N-1} e^{-i2k\pi j/N} = 0,$$

completing the proof of the corollary.

We remark here that the above results also hold for the case where the support of $f(x)$ is in $[a, b]$.

From the conditions of Theorem 1, we have assumed that the points of discontinuity of $f(x)$ are equally distributed and they coincide with some nodes x_j. For practical problems, we have to consider the case in which the points of discontinuity are located at any place. For convenience, we assume that $f(x)$ has only one point of discontinuity inside the interval (0,1), denoted as z, and $x_p < z < x_p + 1/N, 0 < p < N - 1$. Now, we will use new partitions of nodes so that the derivative of $f(x)$ exists on every subinterval. Let

$$0 = x_0 < x_1 < \cdots < x_p < z < x_{p+2} < \cdots < x_{N-1} < x_N = 1, \tag{23}$$

$$\Delta x_j = x_{j+1} - x_j = \Delta x = \frac{1}{N}, j \neq p, p+1, \Delta x_p = z - x_p, \Delta x_{p+1} = x_{p+2} - z, \tag{24}$$

and

$$f_j = f(\eta_j),\ j = 0, \ldots, N-1 \text{ with } \eta_j = x_j + \delta_j, \tag{25}$$

where $0 \leq \delta_j = \delta \leq \Delta x, j = 0, \ldots, N-1, j \neq p, p+1, 0 \leq \delta_p \leq \Delta x_p$ and $0 \leq \delta_{p+1} \leq \Delta x_{p+1}$ are some constants.

We get a new approximate relation between $\hat{f}_k$ and $\tilde{f}_k$ as follows

Theorem 2. Suppose that the function $f(x)$ satisfies Assumptions 1-3, and $f(x)$ only has one interior point of discontinuity z. The partitions of nodes of interval [0,1] and $\{f_j\}_0^{N-1}$ are defined in (23) - (25) respectively. Then

$$|\hat{f}_k - a_k \tilde{f}_k - (f_p - f_{p+1})\hat{g}_k| \leq C(f)\Delta x \tag{26}$$

where

$$\hat{g}_k = \begin{cases} z - x_{p+1}, & k = 0, \\ \frac{1}{-i2\pi k}(e^{-i2\pi z k} - e^{-i2\pi x_{p+1} k}), & k \neq 0, \end{cases} \tag{27}$$

and $C(f)$ is a nonnegative constant depending upon f. $\{a_k\}$ is the same as that in Theorem 1.

Proof:The proof is similar to that of Theorem 1. We first consider the case that $k \neq 0$. We use the rectangular rule for the approximation of integral to get

$$\hat{f}_k = \sum_{j=0, j\neq p, p+1}^{N-1} \int_{x_j}^{x_{j+1}} f(x)e^{-i2k\pi x}dx + \int_{x_p}^{z} f(x)e^{-i2k\pi x}dx + \int_{z}^{x_{p+2}} f(x)e^{-i2k\pi x}dx$$

$$= \sum_{j=0, j\neq p, p+1}^{N-1} f_j \int_{x_j}^{x_{j+1}} e^{-i2k\pi x}dx + f_p \int_{x_p}^{z} e^{-i2k\pi x}dx + f_{p+1} \int_{z}^{x_{p+2}} e^{-i2k\pi x}dx + e_k(\Delta x),$$

where $e_k(\Delta x)$ is the error term (we observe that this error depends on $2\Delta x$) . To use the results in Theorem 1, we rewrite the equality above as

$$\hat{f}_k = \sum_{j=0}^{N-1} f_j \int_{x_j}^{x_{j+1}} e^{-i2k\pi x}dx - f_p \int_{z}^{x_{p+1}} e^{-i2k\pi x}dx + f_{p+1} \int_{z}^{x_{p+1}} e^{-i2k\pi x}dx$$

According to Theorem 1, we have

$$\hat{f}_k = a_k \tilde{f}_k + (f_p - f_{p+1})\hat{g}_k + e_k(\Delta x) \tag{28}$$

Similarly, we can easily get the estimate for $e_k(\Delta x)$

$$|\int_{x_p}^{z} (f(x) - f_p)e^{-i2k\pi x}dx| \leq \int_{x_p}^{z} \sup_{\xi}|f^{'}(\xi)||(x - \eta_p)|dx \leq \frac{1}{2}C(z - x_p)^2 \leq \frac{1}{2}C(\Delta x)^2,$$

and

$$|\int_{z}^{x_{p+2}} (f(x) - f_{p+1})e^{-i2k\pi x}dx| \leq \int_{z}^{x_{p+2}} \sup_{\xi}|f^{'}(\xi)||(x - \eta_{p+1})|dx \leq \frac{1}{2}C(x_{p+2} - z)^2 \leq 2C(\Delta x)^2,$$

So, we have

$$|e_k(\Delta x)| = |\hat{f}_k - a_k\tilde{f}_k - (f_p - f_{p+1})\hat{g}_k| \le \sum_{j=0, j\neq p,p+1}^{N-1} \int_{x_j}^{x_{j+1}} |f(x) - f_j|dx$$
$$+ \int_{x_p}^{z} |f(x) - f_p|dx + \int_{z}^{x_{p+2}} |f(x) - f_{p+1}|dx \tag{29}$$
$$\le (N-1)\tfrac{1}{2}C(\Delta x)^2 + 2c(\Delta x)^2 \equiv C(f)\Delta x,$$

In the case that $k = 0$, we have that

$$\int_{x_{p+1}}^{z} dx = z - x_{p+1} = \hat{g}_0 \tag{30}$$

Following the proof for the case $k \neq 0$, we can get the same estimate (29) with $a_0 = 0$. Thus we complete the proof of the Theorem.

4. Reconstruction Algorithms

Having established an approximate relationship between the discrete Fourier transform and the Fourier transform of the function $f(x)$ in the previous section, we can easily recover the discrete set $\{f_j, j = 0, 1 \ldots, N-1\}$ of the function $f(x)$ from the Fourier transform of $f(x)$ with frequency k for $k = -N/2, \cdots, N/2 - 1$. We will present two algorithms for the cases in which $f(x)$ satisfies the conditions of Theorem 1 and 2 respectively. If $f(x)$ satisfies the conditions of Theorem 1, then, we have

Algorithm 1. Given $\{\hat{f}(k), k = -N/2, \ldots, N/2 - 1\}$.

Step 1. Set

$$\tilde{f}_k := \sigma_k \hat{f}_k \text{ for } k = -N/2, \cdots, N/2 - 1,$$

where σ_k satisfies (19).

Step 2. Evaluate

$$Rf_j = \sum_{k=-N/2}^{N/2-1} \tilde{f}_k e^{i2k\pi\frac{j}{N}} \text{ for } j = 0, \ldots, N-1$$

using the IFFT, where $\{Rf_j, j = 0, \ldots, N-1\}$ is the reconstructed function at $\{\eta_j, j = 0, \ldots, N-1\}$.

We only need N multiplications for step 1 and $O(N \log_2 N)$ for the IFFT operations in Step 2, so the amount of computation in this algorithm is not large. If $f(x)$ satisfies the conditions of Theorem 2, then, we apply formula (28), so, we have

$$\sigma_k \hat{f}_k \approx \tilde{f}_k + (f_p - f_{p+1})\sigma_k \hat{g}_k, k = -N/2, \ldots, N/2 - 1$$

Denoting the inverse Fourier transform of $\{\sigma_k \hat{f}_k\}_{-N/2}^{N/2-1}$ and $\{\sigma_k \hat{g}_k\}_{-N/2}^{N/2-1}$ by $\{h_j\}_0^{N-1}$ and $\{g_j\}_0^{N-1}$ respectively , we obtain

$$h_j = f_j + (f_p - f_{p+1})g_j, j = 0, \ldots, N-1 \tag{31}$$

We can get $\{f_j\}_0^{N-1}$ by solving the set of equations (31). The algorithm is described in the following.

Algorithm 2. Given $\{\hat{f}(k), k = -N/2, \ldots, N/2 - 1\}$ and $\{\hat{g}(k), k = -N/2, \ldots, N/2 - 1\}$

Step 1. Set

$$\tilde{h}_k := \sigma_k \hat{f}_k \text{ for } k = -N/2, \cdots, N/2 - 1,$$

$$\tilde{g}_k := \sigma_k \hat{g}_k \text{ for } k = -N/2, \cdots, N/2 - 1,$$

where σ_k satisfies (19).

Step 2. Evaluate

$$h_j = \sum_{k=-N/2}^{N/2-1} \tilde{h}_k e^{i2k\pi \frac{j}{N}} \text{ for } j = 0, \ldots, N-1$$

$$g_j = \sum_{k=-N/2}^{N/2-1} \tilde{g}_k e^{i2k\pi \frac{j}{N}} \text{ for } j = 0, \ldots, N-1$$

using the IFFT.

Step 3. Find the solution of equations (31) as follows

3.1

$$\begin{cases} (1 - g_p)Rf_p - g_p Rf_{p+1} & = h_p \\ g_{p+1}Rf_p + (1 - g_{p+1})Rf_{p+1} & = h_{p+1} \end{cases} \tag{32}$$

3.2

$$Rf_j = h_j - (Rf_p - Rf_{p+1})g_j, j = 0, \ldots, N-1, j \neq p, p+1. \tag{33}$$

We only need $2N$ multiplications for step 1,$O(Nlog_2N)$ for 2 IFFT operations in step 2, and a few operations for finding solution (32) and (33) in step 3, so the amount of computation in this algorithm is the same order of Algorithm 1. If $f(x)$ has more than one point of discontinuity which have the same characteristic with z, we can get a similar algorithm. In that case, we will have more IFFT operations in step 2 and find solution of a set of complicated equations in step 3. Of course, we can evaluate it by iteration method .

Using the same idea, we can get a reconstruction algorithm for multi-dimensional functions.

5. Numerical Examples

In this section, we show the results from several numerical experiments to illustrate the behavior the algorithms. All the computations were performed using MATLAB on a Sun Workstation at the Applied Mathematics Department, State University of Campinas, SP, Brazil. The machine precision is $u \sim 10^{-16}$.

For the first three examples, we perform computations by using Algorithm 1 with $N =$ 64, 128, 256. In the last two examples, we performed computations by using Algorithm 1 and 2 respectively with $N = 128$. We compared the pointwise error of reconstruction methods using different window functions σ_k, $\sigma_k^{(1)}$, $\sigma_k^{(2)}$ and $\sigma_k^{(3)}$. We also calculate the mean-square errors defined as:

$$e = \sqrt{\frac{1}{N}\sum_{j=0}^{N-1} |f_j - Rf_j|^2} \tag{34}$$

Example 1. Function $f_1(x)$:

$$f_1(x) = \begin{cases} x, & x \in [0,1], \\ 0, & x \notin [0,1]. \end{cases} \tag{35}$$

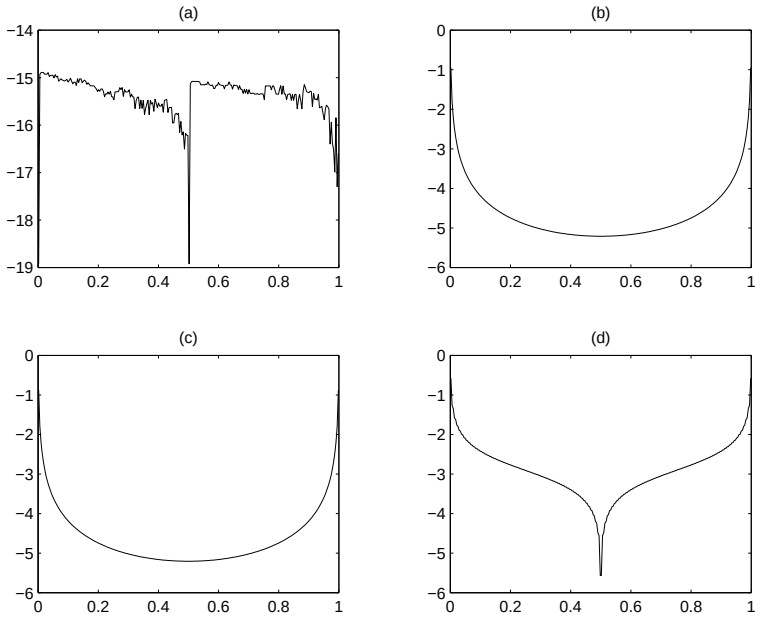

Figure 1: The graphic of the pointwise reconstructed error $log_{10}|Rf_1(x) - f_1(x)|$ with $N = 256$. (a) - (d) are respectively for $\{\sigma_k\}$ and $\{\sigma_k^{(m)}, m = 1, 2, 3\}$.

Notice that in the interval $(0,1)$, $f_1(x)$ is analytic, $f_1(0) \neq f_1(1)$.

Fig. 1 ,(a) - (d) shows the graphics of the pointwise errors by using the window functions $\{\sigma_k\}$ and $\{\sigma_k^{(m)}, m = 1,2,3\}$respectively with $N = 256$.

From Fig. 1, we see that our reconstruction error is about $O(10^{-16})$ caused by roundoff error because $f_1(x)$ is linear in [0,1], which verifies Corollary 2.

Table 1 lists the mean-square errors for reconstruction methods by using different window functions with $N = 64,\ 128,\ 256$.

Table 1. Mean-square error for $f_1(x)$

N	σ_k	$\sigma_k^{(1)}$	$\sigma_k^{(2)}$	$\sigma_k^{(3)}$
64	1.7408×10^{-16}	$2.0253\ \times10^{-2}$	2.3987×10^{-2}	4.8369×10^{-2}
128	$2.0529\ \times10^{-16}$	1.4317×10^{-2}	$1.6957\ \times10^{-2}$	$3.4700\ \times10^{-2}$
256	6.0281×10^{-16}	$1.0123\ \times10^{-2}$	$1.1990\ \times10^{-2}$	$2.4717\ \times10^{-2}$

Example 2. Function $f_2(x)$:

$$f_2(x) = \begin{cases} 1, & x \in I \equiv [0,1/4) \cup [1/2,5/8) \cup [3/4,7/8), \\ 0, & \text{otherwise.} \end{cases} \tag{36}$$

Notice that $f_2(x)$ is a step function with 6 points of discontinuity.

In Fig. 2, (a) - (d) are graphics of the pointwise error by using the window functions $\{\sigma_k\}$ and $\{\sigma_k^{(m)}, m = 1,2,3\}$respectively with $N = 256$.

From Fig. 2, we see that our reconstruction error is about $O(10^{-16})$ caused by roundoff error, which verifies Corollary 1.

Table 2 lists the mean-square errors for reconstruction methods by using different window functions with $N = 64,\ 128,\ 256$.

Table 2. Mean-square error for $f_2(x)$

N	σ_k	$\sigma_k^{(1)}$	$\sigma_k^{(2)}$	$\sigma_k^{(3)}$
64	1.1510×10^{-15}	4.9144×10^{-2}	5.8302×10^{-2}	1.1888×10^{-1}
128	1.7342×10^{-15}	3.4986×10^{-2}	4.1457×10^{-2}	8.5176×10^{-2}
256	2.4355×10^{-15}	2.4781×10^{-2}	2.9355×10^{-2}	6.0614×10^{-2}

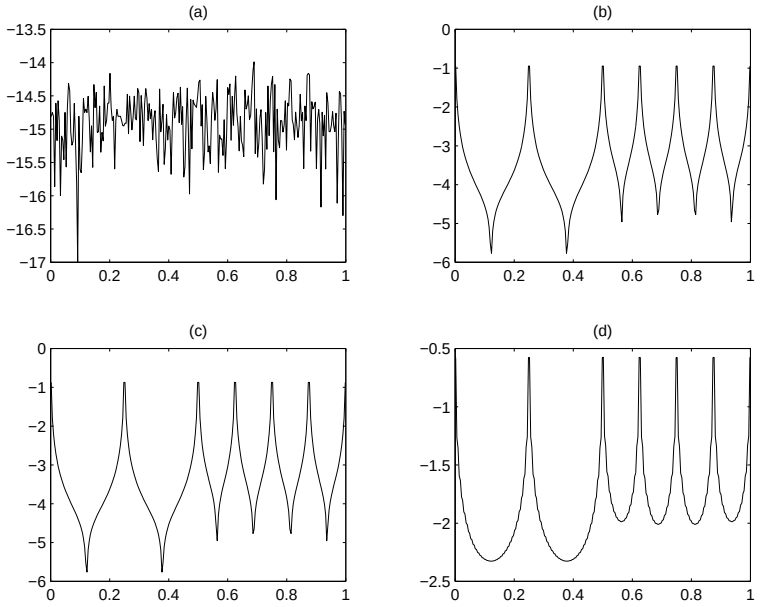

Figure 2: The graphic of the pointwise reconstructed error $log_{10}|Rf_2(x) - f_2(x)|$ with $N = 256$. (a) - (d) are respectively for $\{\sigma_k\}$ and $\{\sigma_k^{(m)}, m = 1, 2, 3\}$.

Example 3. Function $f_3(x)$:

$$f_3(x) = \begin{cases} x^2, & x \in [0,1], \\ 0, & x \notin [0,1]. \end{cases} \tag{37}$$

Notice that in the interval $(0,1)$, $f_3(x)$ is analytic, $f_3(0) \neq f_3(1)$.

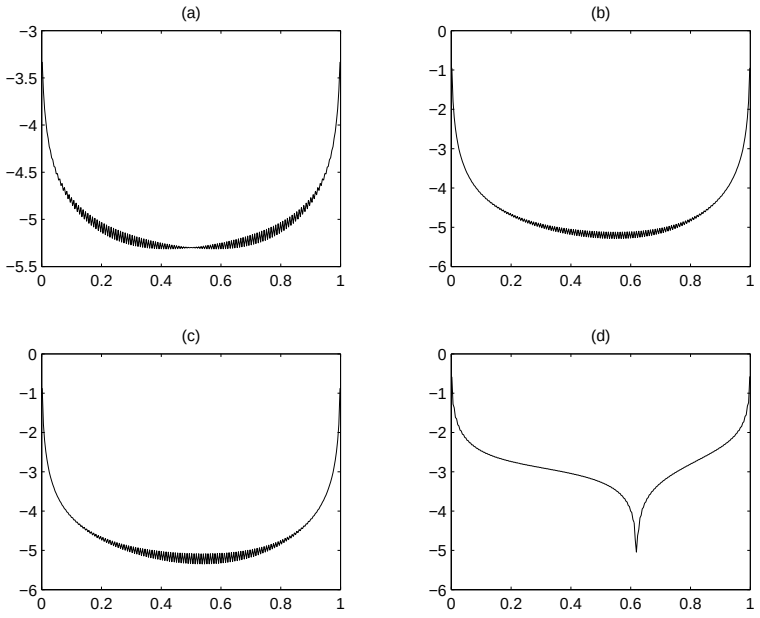

Figure 3: The graphic of the pointwise reconstructed error $log_{10}|Rf_3(x) - f_3(x)|$ with $N = 256$. (a) - (d) are respectively for $\{\sigma_k\}$ and $\{\sigma_k^{(m)}, m = 1,2,3\}$.

Fig. 3 shows the graphic of the original function. In Fig. 6, (a) - (d) are graphics of the pointwise error by using the window functions $\{\sigma_k\}$ and $\{\sigma_k^{(m)}, m = 1,2,3\}$respectively with $N = 256$.

From Fig. 3, we see that our reconstructed error using the window function σ_k at the points near $x = 0$ and $x = 1$ are much smaller than using any other window functions. So we can greatly reduce the oscillations of the Gibbs phenomenon in the reconstructed function.

Table 3 lists the mean-square errors for reconstruction methods by using different window functions with $N = 64,\ 128,\ 256$.

Table 3. Mean-square error for $f_3(x)$

N	σ_k	$\sigma_k^{(1)}$	$\sigma_k^{(2)}$	$\sigma_k^{(3)}$
64	4.1411×10^{-4}	2.0253×10^{-2}	2.3987×10^{-2}	4.8442×10^{-2}
128	1.4665×10^{-4}	1.4317×10^{-2}	1.6957×10^{-2}	3.4727×10^{-2}
256	5.1891×10^{-5}	1.0123×10^{-2}	1.1990×10^{-2}	2.4727×10^{-2}

Example 4. Function $f_4(x)$:

$$f_4(x) = \begin{cases} 0, & x \in [0, 0.5 + 1/256], \\ 1, & x \notin [0, 0.5 + 1/256]. \end{cases} \tag{38}$$

We divide interval [0,1] into 128 equal subintervals ($N = 128$), so this example satisfies the conditions of Theorem 2.

Fig. 4 shows the graphic of the original function and the reconstructions. In Fig. 5, (a) - (d) are graphics of the pointwise error by using Algorithm 1 with four window functions $\{\sigma_k\}$ and $\{\sigma_k^{(m)}, m = 1, 2, 3\}$respectively and (e) is for Algorithm 2 with window function $\{\sigma_k\}$. From Fig. 5, we see that the reconstruction errors are more or less the same by using Algorithm 1 with four window functions $\{\sigma_k\}$ and $\{\sigma_k^{(m)}, m = 1, 2, 3\}$, and their mean-square errors are $4.9869 \times 10^{-2}, 4.7283 \times 10^{-2}, 4.7745 \times 10^{-2}$and 5.8743×10^{-2} respectively. But, the reconstruction error is abour $O(10^{-16})$ caused by roundoff error by using Algorithm 2 with our window function, the mean-square error of which is 1.1654×10^{-15}.

Example 5. Function $f_5(x)$:

$$f_5(x) = \begin{cases} x^2, & x \in [0, 0.5 + 1/256], \\ cos(x), & x \notin [0, 0.5 + 1/256]. \end{cases} \tag{39}$$

Like Example 4, we divide interval [0,1] into 128 equal subintervals ($N = 128$).

Fig. 6 shows the graphic of the original function and the reconstructions. In Fig. 10, (a) - (d) are the graphics of the pointwise error by using Algorithm 1 with four window functions $\{\sigma_k\}$ and $\{\sigma_k^{(m)}, m = 1, 2, 3\}$ respectively and (e) is for Algorithm 2 with window function $\{\sigma_k\}$. From Fig. 7, we see that the reconstruction errors are more or less the same by using Algorithm 1 with four window functions $\{\sigma_k\}$ and $\{\sigma_k^{(m)}, m = 1, 2, 3\}$, and

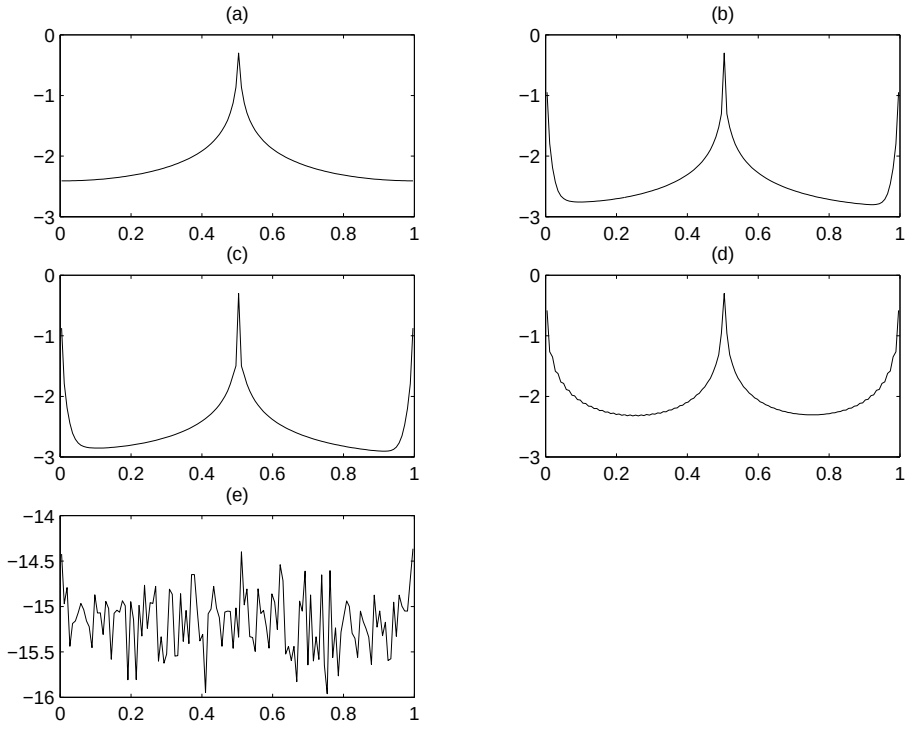

Figure 4: The graphic of the pointwise reconstructed error $log_{10}|Rf_4(x) - f_4(x)|$ with $N = 128$. (a) - (d) are respectively for using Algorithm 1 with $\{\sigma_k\}$ and $\{\sigma_k^{(m)}, m = 1, 2, 3\}$. (e) is for using Algorithm 2 with $\{\sigma_k\}$.

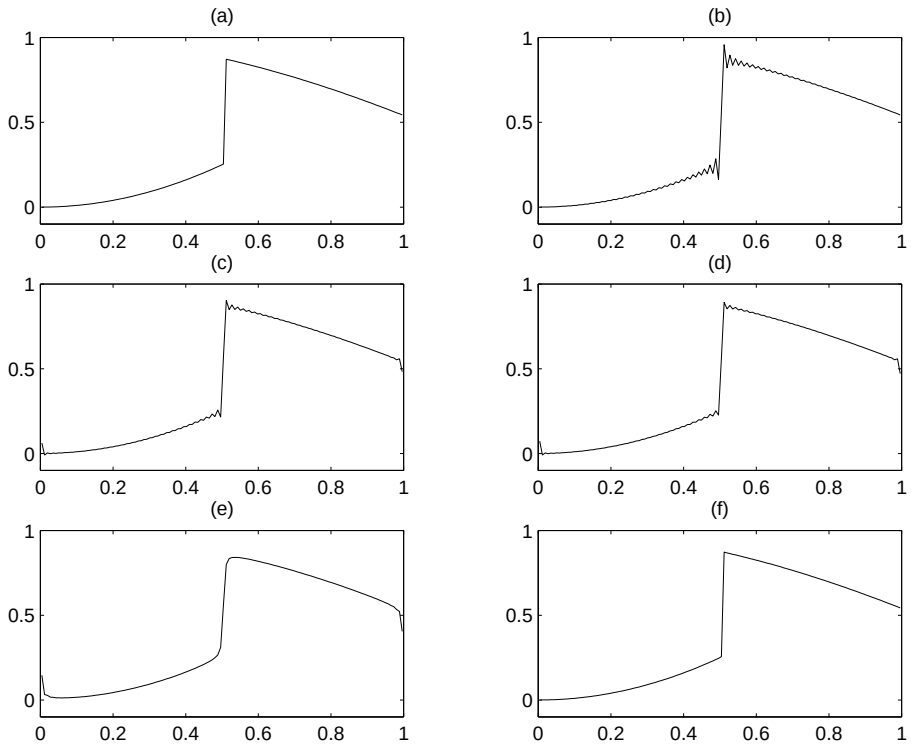

Figure 5: The original and reconstructed gragpic of $f_5(x)$. (a) is for orginal graphic, (b) - (e) are for using Algorithm 1 with $\{\sigma_k\}$ and $\{\sigma_k^{(m)}, m = 1, 2, 3\}$ respectively. (f) is for using Algorithm 2 with $\{\sigma_k\}$.

their mean-square errors are $3.0958 \times 10^{-2}, 2.8930 \times 10^{-2}, 2.9071 \times 10^{-2}$,and 3.4523×10^{-2} respectively. But, by using Algorithm 2 with our window function, the reconstruction error at the point near $x = 0.5 + 1/256$ is much smaller than using Algorithm 1 with four window functions, the mean-square error of which is 2.0141×10^{-4}. It shows that we can greatly reduce the oscillations of the Gibbs phenomenon in the reconstructed function.

The above numerical examples show that the window function σ_k introduced in this paper is the best one for reconstructing a function having compact support which has points of discontinuity and/or is not periodic over the interval of support. Of course, we have to use Algorithm 1 and 2 respectively according to the different points of discontinuity of $f(x)$.

5. Conclusion

In this paper, we have derived a new relation between the discrete Fourier transform of a discrete sampling set of compactly supported function and its Fourier transform and provided an error estimation. From this relation we have obtained a new window function σ_k which is much better than any known window function to reduce oscillations in the Gibbs phenomenon. We have proposed a new efficient algorithm to reconstruct the original function from the discrete sampling of its Fourier transform, which can adopt the fast Fourier transform and has much better accuracy than those in the literature. Several numerical experiments have also been provided to demonstrate the results.

References

[1] M. Bertero, C. Demol, and E.R. Pike, " Linear inverse problems with discrete data, I: General formulation and singular system analysis", Inverse Probl., Vol. 1, pp. 301-330, 1985.

[2] R.P. Boas, Entire Functions, Academic Press, New York, 1954.

[3] C. Canuto, M.Y. Hussaini, A. Quarteroni and T. A. Zang, Spectral Methods in Fluid Dynamics, Springer-Verlag, 1988.

[4] W. K. Cheung and R. M. Lewitt, "Modified Fourier reconstruction method using shifted transform samples", Phys. Med. Biol., Vol. 36, No.2, pp. 269-277, 1991.

[5] D. Gottlieb and S. Orszag, Numerical Analysis of Spectral Methods: Theory and Applications, SIAM, Philadelphia, PA, 1977.

[6] D. Gottlieb, C.W. Shu, A. Solomonoff and H. Vandeven, " On the Gibbs phenomenon I: recovering exponential accuracy from the Fourier partial sum of the a nonperiodic analytic function", J. Comput. Appl. Math., Vol. 43,pp. 81-98, 1992.

[7] G. Hammerlin, K.-H. Hoffmann, Numerical Mathematics, Springer-Verlag, 1991.

[8] G. Hamming, Numerical Methods for Scientists and Engineers, 2nd Edit., McGraw-Hill, New York, 1973.

[9] G.T. Herman, Image Reconstruction from Projections: the Fundamentals of Computerized Tomography, Academic Press, New York, 1980.

[10] A. K. Jain, Fundamentals of Digital Image Processing, Englewood Cliffs, NJ: Prentice-Hall, 1989.

[11] A. C. Kak and M. Slaney, Principles of Computerized Tomographic Imaging, New York: IEEE Press, 1988.

[12] E.D. Kolaczyk, " A wavelet shrinkage approach to tomographic image reconstruction", J. Am. Statist. Assoc., vol. 91, 1996.

[13] F. Natterer, The Mathematics of Computerized Tomography, New York: Wiley, 1985.